Qi, Pengfei ; Pichler, Thomas

Sequential and simultaneous adsorption of Sb(III) and Sb(V) on ferrihydrite: Implications for oxidation and competition

Journal Article as: peer-reviewed accepted version (Postprint)

DOI of this document*(secondary publication): https://doi.org/10.26092/elib/3214

Publication date of this document: 15/08/2024

* for better findability or for reliable citation

Recommended Citation (primary publication/Version of Record) incl. DOI:

Pengfei Qi, Thomas Pichler, Sequential and simultaneous adsorption of Sb(III) and Sb(V) on ferrihydrite Implications for oxidation and competition, Chemosphere, Volume 145, 2016, Pages 55-60, ISSN 0045-6535, https://doi.org/10.1016/j.chemosphere.2015.11.057.

Sequential and simultaneous adsorption of Sb(III) and Sb(V) on ferrihydrite: Implications for oxidation and competition

Pengfei Qi*, Thomas Pichler

Geochemistry & Hydrogeology, Department of Geosciences, University of Bremen, Klagenfurter Straße, 28359 Bremen, Germany

HIGHLIGHTS

- The simultaneous adsorption and oxidation of Sb(III) was confirmed by the appearance of Sb(V) in the solution.
- Competition occurred between the newly formed Sb(V) and the original Sb(III).
- Sb(III) adsorption was not affected by Sb(V) while Sb(V) adsorption was inhibited by Sb(III).
- Sb(V) should be the dominant species in aquatic environment.

Keywords:
Antimony(III,V)
Ferrihydrite
Adsorption
Oxidation
Competition

1. Introduction

Antimony (Sb) is a naturally occurring element of growing environmental concern. Large quantities of Sb have been released into the environment as a result of both natural and anthropogenic

---

* Corresponding author.
E-mail address: pengfei@uni-bremen.de (P. Qi).

processes such as rock weathering, soil runoff, Sb mining and smelting (Filella et al., 2002, 2007). Inorganic Sb exists primarily as the pentavalent species (Sb(V)) in oxic systems and as the trivalent species (Sb(III)) in anoxic systems (Vink, 1996). Its toxicity, adsorption behavior and other chemical properties are similar to that of arsenic (As) (Gebel, 1997; Wilson et al., 2010). However, due to a lower abundance in the environment and the relatively low solubility of most Sb compounds, it is less studied compared to As.

The mobility of Sb is susceptible to redox changes, such as oxidation of Sb(III) to Sb(V) which can be effectively initiated in aerated Fe(III)–H_2SO_4 solutions, by H_2O_2, and by manganese and iron oxyhydroxides (Belzile et al., 2001; Quentel et al., 2004; Leuz and Johnson, 2005; Asta et al., 2012). A recent study suggested that oxidation of Sb(III) occurred after Sb(III) was adsorbed on goethite and thus any Sb(V) in the aqueous phase was a result of desorption from the surface (Xi et al., 2013). Belzile et al. (2001) reported the complete oxidation of Sb(III) by synthetic iron oxyhydroxides within six days. Another study indicated that Sb(III) adsorbed on goethite was partly oxidized at pH 3, 5, 9 and 9.7 within seven days (Leuz et al., 2006b). Xi et al. (2014)) also reported significant oxidation of Sb(III) to Sb(V) under certain experimental conditions during the adsorption of Sb(III) on kaolinite.

Hydrous ferric oxides (HFO), such as ferrihydrite are recognized as effective solid phases for the adsorption and attenuation of Sb in anthropogenic and geogenic systems (Craw et al., 2004; Ahmed et al., 2006; Xi et al., 2013). However, the assessment of Sb(III) adsorption by HFO is complicated because adsorption and oxidation of Sb(III) occur more or less simultaneously. The newly formed Sb(V) could behave differently than the original Sb(III) in solution. Currently next to nothing is known about the mobility of this Sb(V) and its interaction with the remaining Sb(III). Thus Sb(III) adsorption remains somewhat ambiguous and particularly the competition between the two Sb species need further investigation.

Here we present new data for Sb(III) adsorption experiments focusing on Sb speciation analyses in the supernatant following adsorption. The key objective was to examine the kinetics of Sb speciation at varying Fe/Sb molar ratios and pH. In addition, the competition between the two Sb species for adsorption sites as a function of pH in binary systems was evaluated.

2. Experimental section

2.1. Reagents and materials

All chemicals were of analytical grade. Two types of Sb(III) stock solutions were prepared by dissolving potassium antimonyl tartrate ($C_8H_4K_2O_{12}Sb_2 \cdot 3H_2O$, Sigma–Aldrich) in de-ionized distilled (DDI) water or by dissolving antimony trioxide (Sb_2O_3, Aldrich) in 2 M HCl. Unfortunately the solubility of the latter is low and thus the dissolution of Sb_2O_3 had to be performed in highly concentrated acid solutions. Despite the difference in aqueous complexing, antimony tartrate anions and $Sb(OH)_3$ behave similar (Thanabalasingam and Pickering, 1990) and both form inner-sphere complexes during adsorption (Watkins et al., 2006; Xi et al., 2011; Verbinnen et al., 2013; Vithanage et al., 2013). This was once more confirmed prior to conducting the experiments and their adsorption onto ferrihydrite was found to be similar (Fig. S1). Thus the more soluble potassium antimonyl tartrate was used in the adsorption experiments since it was necessary to evaluate the removal efficiency of Sb at high concentrations commonly found in water samples influenced by mining activities (Hiller et al., 2012). Sb(V) stock solutions were prepared by dissolving potassium hexahydroxoantimonate (H_6KO_6Sb, Fluka) in DDI water.

Ferrihydrite was synthesized following an established method (Qi and Pichler, 2014), by adding dropwise and under constant stirring a 1 M solution of KOH (Sigma–Aldrich, Germany) to 500 mL of 0.2 M $Fe(NO_3)_3 \cdot 9H_2O$ (Alfa Aesar, Germany), until the pH increased to 7.4 ± 0.1. The precipitated material was then washed with DDI water, freeze-dried, ground and stored in polyethylene bags in the refrigerator. X-ray diffraction analysis of the material confirmed two-line ferrihydrite. The surface area of freeze-dried ferrihydrite was analyzed by the BET (Brunauer–Emmett–Teller) method and found to be 120 m^2/g.

2.2. Experimental procedure

All experiments were carried out at room temperature, with a background electrolyte of 0.01 M NaCl. In the individual adsorption experiments of Sb(III), the Sb(III) working solutions were mixed with ferrihydrite in 100 mL conical flasks with plugs, and the pH of the suspensions was adjusted to 7.0 ± 0.2 with HCl or NaOH. The molar ratios of Fe to Sb were 8, 100 and 500. Suspensions were capped and maintained under constant stirring. Aliquots of suspensions were collected after 1, 5, 24, 48, 96 and 120 h and filtered immediately through syringe filters with a pore size of 0.25 μm. The samples were preserved using a combination of 0.2 M EDTA and HCl and stored at 4 °C in the dark (Wu and Pichler, 2015). To test for the possibility of oxidation by atmospheric oxygen during the experiment a blank Sb(III) solution was prepared and analyzed at the same time intervals. To study the influence of pH the same experimental setup was used at pH 3.8 ± 0.2 and pH 9.0 ± 0.2 at a Fe to Sb ratio of 100. The samples were collected and analyzed for Sb speciation at the same time intervals of 1, 5, 24, 48, 96 and 120 h. The percentage of Sb(III) adsorbed onto ferrihydrite was calculated according to the following equation:

$$\%\ \mathrm{Sb(III)adsorbed} = \frac{[\mathrm{Sb(III)}]_{tot} - [\mathrm{Sb(III)}]_{aq} - [\mathrm{Sb(V)}]_{aq}}{[\mathrm{Sb(III)}]_{tot}} \times 100\%$$

To asses if Sb(III) converted to Sb(V) after adsorption, three replicates of 5 mL ferrihydrite suspensions were collected at the end of the experiments (pH 3.8 and 9) and dissolved in 2 M EDTA and 6 M HCl. After complete dissolution of ferrihydrite the samples were diluted to 20 mL with DDI water and filtered for Sb speciation analyses. A combination of EDTA and HCl was chosen, because HCl can dissolve ferrihydrite without a change in redox conditions and EDTA is known to complex Sb(III) in a way that prevents oxidation (Daus and Wennrich, 2014).

Individual and co-adsorption experiments as a function of pH were performed in 50 mL tubes, by adding either Sb(III) or Sb(V) or a combination of both to a ferrihydrite suspension. The concentrations of each Sb species at each pH in the single and binary systems were identical with a concentration of 50 mg/L, and the adsorbent dosage was 0.5 g/L. The pH was adjusted from 4 to 10, and the suspensions were continuously shaken for 24 h in case of long time contact promoting oxidation interference. At the end of the experiment the suspensions were filtered and the supernatant was analyzed for total Sb concentration and Sb speciation. These experiments were performed in triplicates and one blank was prepared for each pH studied.

2.3. Analytical methods

The Sb speciation was determined by hydride generation-atomic fluorescence spectroscopy (HG-AFS) on a PSA 10.055 Millennium Excalibur system. Prior to analysis the two Sb species were separated chromatographically in an anion exchange column (Hamilton PRP-X100) using 20 mM EDTA at pH 4.7 as the mobile phase. The detection limits for Sb(III) and Sb(V) were 0.02 and

0.2 μg/L, respectively.

The total Sb concentration was measured using inductively coupled plasma-optical emission spectrometry (ICP-OES), and the detection limit was 0.02 mg/L. If Sb concentration were below the detection limit of ICP-OES, total Sb was determined by HG-AFS by reducing Sb(V) to Sb(III) with potassium iodide (KI) and ascorbic acid. The limit of detection of that method was 0.01 μg/L.

3. Results

3.1. *Effect of Fe/Sb ratios*

The data for Sb speciation in the supernatant of the Sb(III) adsorption experiments are shown in Figs. 1 and 2 as well as the adsorption percentage of Sb(III) as a function of time. At a Fe/Sb ratio of 500, the concentration of Sb(III) in the aqueous phase decreased from 2 mg/L to less than 0.02 mg/L (Fig. 1a), indicating almost complete removal of Sb(III) within the first hour of the experiment. However, a small amount of Sb(V) was detected in solution likely due to the oxidation of Sb(III). Previous studies also reported the rapid uptake of Sb(III) and rapid formation of Sb(V) in solution due to the oxidation of Sb(III) for example by manganite (Wang et al., 2012). The newly formed Sb(V) can then be subsequently removed from solution and thus Sb(V) was only detectable for a short period during the experiment. After 96 h, neither Sb(III) nor Sb(V) were detected in the solution and adsorption of Sb(III) was close to 100%. This indicated that the oxidation of Sb(III) to Sb(V) did not affect the overall adsorption behavior of Sb(III) at a high adsorbent to adsorbate ratio, since there were sufficient adsorption sites to adsorb the initial Sb(III) and the newly formed Sb(V).

At the lower Fe/Sb ratio of 100, the adsorption of Sb(III) was found to be less effective than that at the Fe/Sb ratio of 500 (Fig. 1b). After 1 h Sb(V) was observed in the aqueous phase and remained in solution until the end of the experiment. This observation was in contrast to the result of the experiment at a Fe/Sb ratio of 500 where Sb(V) was completely removed by the end of the experiment (Fig. 1a). At the Fe/Sb ratio of 100 only 1.97 mg/L (98.5%) of Sb(III) were removed from the aqueous phase after 120 h. Of the remaining of 0.03 mg/L (1.5%) Sb, approximately 0.025 mg/L (1.25%) were Sb(V) and 0.005 mg/L (0.25%) were Sb(III). That indicated that Sb(III) was preferentially adsorbed onto ferrihydrite at the lower Fe/Sb ratio (i.e., less adsorption sites per adsorbate) at neutral pH, leaving some Sb(V) which formed due to the oxidation of Sb(III) in the aqueous phase after all possible adsorption sites were occupied. At the even lower Fe/Sb ratio of 8 and at a high initial concentration of 40 mg/L, this effect was magnified, generating substantially more Sb(V) in solution. The concentration of Sb(V) decreased with time having a low peak at 24 h but then increased to a final value of more than 0.6 mg/L (1.5%) at 120 h (Fig. 2b). That indicated that the oxidation of Sb(III) and the fate of generated Sb(V) was dependent on Fe/Sb molar ratios.

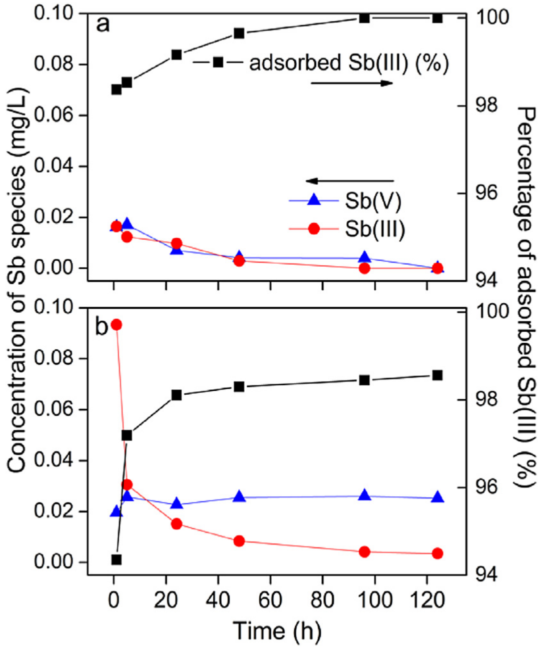

Fig. 1. Sb speciation in the supernatant during Sb(III) adsorption experiments and the adsorption percentage of Sb(III) as a function of time at a Fe/Sb molar ratio of 500 (a) and at a ratio of 100 (b) (volume of suspensions: 100 mL, initial concentration of Sb(III): 2 mg/L, pH: 7.0 ± 0.2).

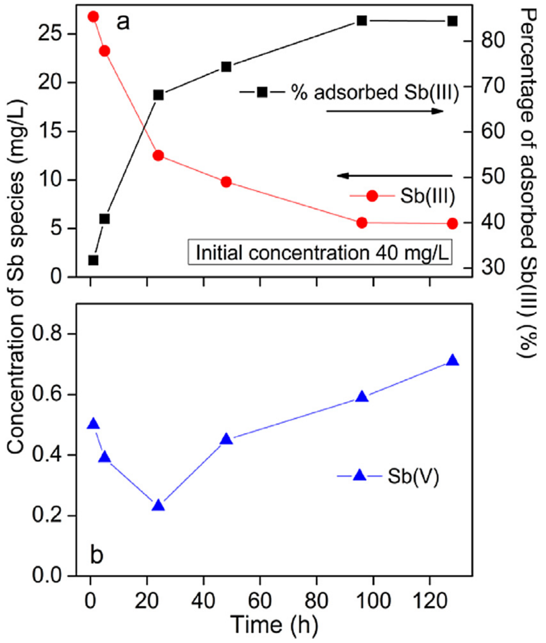

Fig. 2. Sb speciation in the supernatant during Sb(III) adsorption experiments and the adsorption percentage of Sb(III) as a function of time. (a): Concentration of Sb(III) in solution and Sb(III) adsorption percentage as time; (b) Concentration of Sb(V) in solution (volume of suspensions: 100 mL, Fe/Sb molar ratio: 8, pH: 7.0 ± 0.2).

3.2. *Effect of pH*

The effect of pH on Sb speciation in the supernatant during the Sb(III) adsorption experiments and the adsorption behavior of Sb(III) are shown in Fig. 3. The molar ratio of Fe/Sb was 100 and the initial concentration of Sb(III) was 2 mg/L. At pH 3.8 Sb(V) was initially detected in the aqueous phase, but immediately decreased to below detection after 48 h (Fig. 3a). At pH 7 approximately 0.025 mg/L (1.25%) of Sb(V) were detected, which remained constant throughout the experiment (Fig. 3b). At pH 9 the initial concentration of Sb(V) was lower than the other two experiments (Fig. 3c), but continuously increased until reaching a maximum of 0.047 mg/L (2.35%) after 48 h, and followed by a slight decrease to just below 0.04 mg/L (2%) at the end of the experiment (Fig. 3c). The percentages of Sb(III) adsorbed were approximately 100% at pH 3.8, 98.5% at pH 7 and 98% at 9. Thus under acidic conditions the Sb(V), which was formed by Sb(III) oxidation was subsequently removed from solution. However, the newly formed Sb(V) was still present in solutions at neutral and alkaline pH. Meanwhile, the Sb(III) concentration declined constantly until it was below or near detection

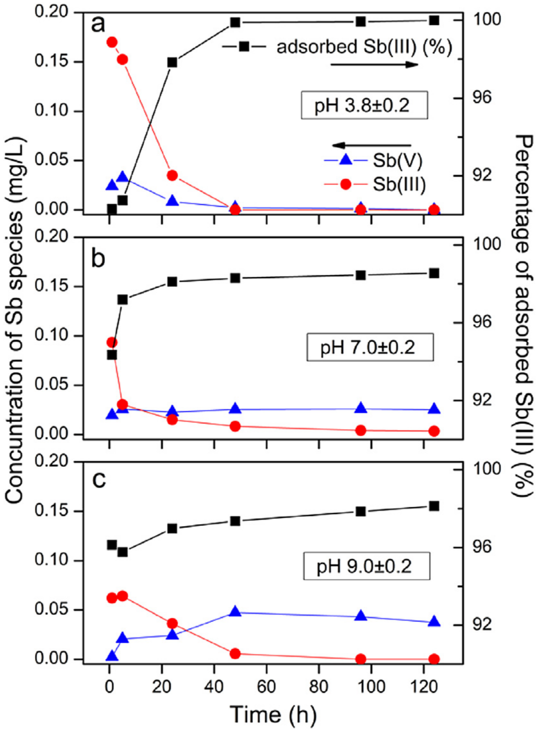

Fig. 3. Sb speciation in the supernatant during Sb(III) adsorption experiments and the adsorption percentage of Sb(III) as a function of time at different pH values (volume of suspensions: 100 mL, Fe/Sb molar ratio: 100, initial concentration of Sb(III): 2 mg/L).

after 96 h at each of the 3 pH settings (Fig. 3). The Sb(III) oxidation was stronger under alkaline conditions and the mobility of formed Sb(V) in solutions was affected by the pH. Buschmann et al. (2005) found a similar degree of pH dependence for photo-induced oxidation of Sb(III) on humic acid.

3.3. *Dissolution of ferrihydrite suspensions after adsorption*

The ferrihydrite suspensions of the adsorption experiments at pH 3.8 and 9 were dissolved after completion and the results of Sb speciation analyses are presented in Fig. 4. The recovery efficiency was calculated according to the ratio between the total concentration of dissolved Sb species and the initial Sb(III) concentration, which was approximately 88% at a pH of 3.8 and 90% at a pH of 9. The results clearly show that a large amount of the adsorbed Sb(III) was converted to Sb(V) on the surface sites.

3.4. *Sb(III) and Sb(V) adsorption under competitive conditions*

Fig. 5 presents the adsorption behavior of Sb(III) and Sb(V) as a function of pH under individual (single) and competitive (binary) conditions. In the single system, the adsorption of Sb(V) decreased significantly with increasing pH. The strong pH dependence of Sb(V) adsorption and the fact that adsorption was favored at acidic pH were reported for kaolinite and goethite (Leuz et al., 2006b; Xi et al., 2010; Guo et al., 2014). The adsorption behavior of Sb(V) in terms of pH is attributed to the electrostatic attraction between $Sb(OH)_6^-$ and the surface of ferrihydrite (Zhao et al., 2014). The pH dependence of Sb(III) adsorption was less pronounced than that of Sb(V), showing an increase in adsorption to the pH at which adsorption was almost complete (Fig. 5). This was in good agreement with the earlier studies, which showed that Sb(III) adsorption by iron oxides can be optimized over a broad pH range (Leuz et al., 2006b; Guo et al., 2014; Shan et al., 2014).

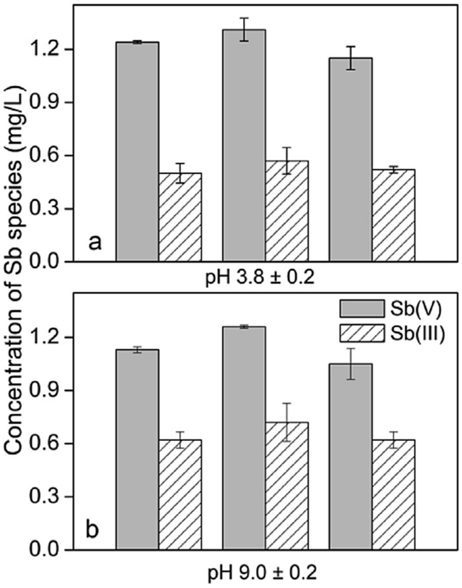

Fig. 4. Speciation analysis for Sb, which was removed from ferrihydrite suspensions at the end of the adsorption experiments at (a) pH 3.8 ± 0.2 and (b) 9.0 ± 0.2 (same experimental conditions as in Fig. 3). Three replicates from each experiment were analyzed. Error bars are the standard deviation of triplicates.

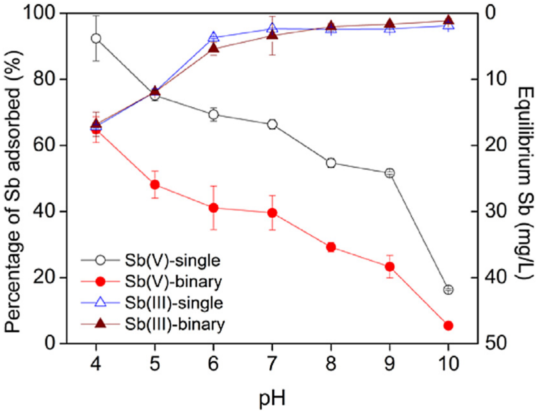

Fig. 5. Sb(III) and Sb(V) adsorption envelopes as a function of pH in single and binary systems respectively (pH from 4 to 10; initial concentration of each Sb species: 50 mg/L; adsorbent dosage: 0.5 mg/L). Error bars are the standard deviation of triplicates.

As seen in the time series experiments (Fig. 2), the amount of Sb(V) formed by Sb(III) oxidation at a high initial Sb(III) concentration seemed to be negligible compared to the initial concentration used during competitive adsorption experiments. The adsorption of Sb(III) in single systems was more or less identical as that observed in binary systems (Fig. 5). On the other hand, the percentage of Sb(V) adsorbed in binary systems decreased by approximately 25% compared to those adsorbed in single systems between pH 4 to 9. Sb(III) adsorption was not affected by the presence of Sb(V), while Sb(III) had an inhibitory effect on the adsorption of Sb(V). Competition took place between Sb(III) and Sb(V), and Sb(III) outcompeted Sb(V). Thus the adsorption of Sb(V) was diminished by the presence of Sb(III) in binary systems.

4. Discussion

4.1. *Implications of oxidation accompanying Sb(III) adsorption*

The Sb(V), which was detected in the supernatant of Sb(III) adsorption experiments showed a different behavior for each of the Fe/Sb ratios and pH values studied. Independent of experimental conditions Sb(V) appeared immediately at the start of each experiment, but subsequently disappeared from solution at a high Fe/Sb ratio (500) or a low pH (Figs. 1a and 3a). While at a lower Fe/Sb ratio of 100 or under non-acidic conditions, the concentration of Sb(V) remained more or less constant with time (Figs. 1b and 3b-c). There are several possible explanations, (1) due to insufficient adsorption sites the newly formed Sb(V) was in competition and Sb(III) showed a stronger affinity, (2) the removal of Sb(V) was significantly affected by an increasing pH or (3) oxidation of Sb(III) on the surface of ferrihydrite. It was reported that Sb(III) adsorbed on goethite was oxidized to Sb(V) and then its release resulted in the observed Sb(V) in the solution (Leuz et al., 2006b; Watkins et al., 2006). However, it cannot be simply inferred that the release of Sb(V) caused the detected Sb(V) in aqueous solution, since both Sb(III) and Sb(V) can be bound strongly to the surface sites by the formation of inner-sphere surface complexes (McComb et al., 2007; Guo et al., 2014). Thus the release of Sb(V) into solution does not occur rapidly and easily in the presence of sufficient adsorption sites or at an acidic pH or in the absence of interferences. According to our observations, the appearance of Sb(V) during Sb(III) adsorption experiments show that Sb(V) is outcompeted by Sb(III) in the case of insufficient adsorption sites or at a basic pH.

4.2. Sb(III) oxidation mechanism

The initial appearance and subsequent disappearance of Sb(V) from the aqueous phase during Sb(III) adsorption indicated a two-step process for the occurrence of Sb(V): (1) oxidation of Sb(III) and (2) removal of formed Sb(V) by ferrihydrite. The speciation analyses of the blank solution of Sb(III) (in the absence of ferrihydrite) did not detect any Sb(V) (Fig. S2), which indicated that dissolved oxygen alone is unlikely to be an oxidant for Sb(III) in our experiments. However, Sb(V) was detected in the supernatant in the presence of ferrihydrite. This suggests that the ferrihydrite surface acts as a catalyst for the oxidation of Sb(III) by dissolved oxygen (Guo et al., 2014) or via an abiotic electron transfer from Sb(III) to Fe(III) (Belzile et al., 2001) to promote oxidation during the adsorption of Sb(III). Moreover, the assumption that adsorbed Sb(III) converted to Sb(V) on the ferrihydrite surfaces was corroborated by the results from the dissolution experiments (Fig. 4). Similar observations were made using XANES, XAFS and XPS to determine the Sb species adsorbed on ferrihydrite, manganite and goethite (Wang et al., 2012; Fan et al., 2014; Guo et al., 2014). These results are similar to those reported for As where the adsorbed As(III) was partially converted to As(V) on the surface of ferrihydrite (Zhao et al., 2011). However, the oxidation of Sb(III) was detected at a lower Fe/Sb molar ratio than the oxidation of As(III). Oxidation of As(III) on ferrihydrite did not occur at low Fe/As ratios or at short contact times (Oscarson et al., 1981; Zhao et al., 2011). This is also supported by the observation that Sb(III) was oxidized more easily at a lower Eh than As(III) and that Sb(V) was a stable oxidation state found over a wide range of Eh in the environment (Mitsunobu et al., 2006). It was reported that the Fe mediated oxidation of Sb(III) proceeded 10 times faster than that of As(III), which was only partly oxidized under the same experimental conditions (Leuz et al., 2006a). The oxidation of Sb(III) by Fe(III) in acid aerated solutions was also found to be faster than that of As(III), and the oxidation rate was highly dependent on the ratio of Fe(III)/Sb(III) or Fe(III)/As(III) (Asta et al., 2012).

4.3. Competition between Sb(III) and Sb(V)

The detection of Sb(V) in the aqueous phase during the Sb(III) adsorption experiments indicated that some Sb(III) was oxidized and that Sb(III) and Sb(V) competed for adsorption sites on ferrihydrite. Particularly since there is evidence that both Sb(III) and Sb(V) can be adsorbed on iron hydroxides via inner-sphere complexes (Guo et al., 2014; He et al., 2015). However, to the best of our knowledge there was no study about the simultaneous removal of Sb(III) and Sb(V) from an aqueous phase via adsorption by ferrihydrite. This could be attributed to the observed oxidation of Sb(III) during adsorption. Another reason could be that Sb-speciation is a rather complex analytical procedure, which is not routinely applied. Nevertheless, a close look at the competitive interaction during simultaneous adsorption of Sb(III) and Sb(V) should further elucidate Sb adsorption in the presence of both Sb species. Our findings indicated that Sb(III) impeded Sb(V) adsorption, while the presence of Sb(V) had no influence on the adsorption of Sb(III) (Fig. 5).

The protonation and deprotonation reactions for the hydroxyl functional group can be written as:

$$\equiv \mathrm{Fe}-OH+\mathrm{H}^{+}\rightarrow \equiv \mathrm{Fe}-\mathrm{OH}_2^{+}(\mathrm{positive}) \tag{1}$$

$$\equiv \mathrm{Fe}-\mathrm{OH}+\mathrm{OH}^{-}\rightarrow \equiv \mathrm{Fe}-\mathrm{O}^{-}+\mathrm{H_2O}(\mathrm{negative}) \tag{2}$$

and thus depending on the pH of the aqueous phase, the surface of ferrihydrite has either a neutral, positive or negative charge. The surface of ferrihydrite has a neutral charge at a pH of approximately 7–8. This pH is called the point of zero charge (PZC) and above this pH the surface has a negative and below this pH a positive charge. In the pH range of 2–11, $\mathrm{Sb(OH)}_6^-$ is the dominant Sb(V) species existing in the solution and thus should be adsorbed preferentially at low pH when the ferrihydrite surface is positively charged. This was observed in the single adsorption experiments, while in the presence of Sb(III) the adsorption of Sb(V) was impeded significantly (Fig. 5). This would indicate that Sb(V) is not attached strongly to the ferrihydrite surface, potentially due to a combination of both outer- and inner-sphere complexes (Wang et al., 2015) instead of inner-sphere complexes only. Sb(III) adsorption, on the other hand was not affected by the presence of Sb(V) nor significantly affected by pH indicating that the uncharged Sb(III) is bound strongly on ferrihydrite by specific inner-sphere binding.

Due to their similar chemical properties, As and Sb should share a similar adsorption behavior. For example, it was reported that As(III) outcompeted As(V) for adsorption sites on ferrihydrite (Qi and Pichler, 2014), similar to what was observed for Sb (Fig. 5). In natural systems, such as hot springs (Pichler et al., 1999), both As and Sb can be present leading to competition during adsorption of different redox states of the same element and between different redox states of two elements. However, no study thus far focused on the simultaneous removal and competitive interactions of As(III,V) and Sb(III,V) in the presence of ferrihydrite. Since As and Sb are recognized pollutants and can occur together in the environment, understanding the simultaneous adsorption of As(III,V) and Sb(III,V) should be the next step.

5. Conclusions

Our study demonstrated that ferrihydrite is an effective adsorbent for Sb(III) and Sb(V) in single and binary systems, with a higher efficiency for Sb(III) than Sb(V). Under competitive conditions, the adsorption of Sb(III) was not affected by the presence of Sb(V) over a wide of pH range. On the other hand Sb(III) had an inhibitory effect on the adsorption of Sb(V). The presence of ferrihydrite not only removed Sb(III) via adsorption, it also catalyzed the oxidation of Sb(III) to Sb(V), while at the same time leading to competition between the newly formed Sb(V) and the original Sb(III) for adsorption sites on ferrihydrite.

These results can also be used to understand the mobility and transport of Sb. In the presence of ferrihydrite and under redox conditions, which would allow the presence of both Sb species, Sb(V) should be the dominant species in aquatic environments, since Sb(III) is adsorbed preferentially.

Acknowledgments

The authors thank Laura Knigge for the ICP-OES analysis and PQ thanks the China Scholarship Council (CSC[2011]305) for funding support. TP acknowledges support by the German Research Foundation (DFG) (INST 144/288-1).

Appendix A. Supplementary data

Supplementary data related to this article can be found at http://dx.doi.org/10.1016/j.chemosphere.2015.11.057.

References

Ahmed, M.F., Ahuja, S., Alauddin, M., Hug, S.J., Lloyd, J.R., Pfatt, A., Pichler, T., Saltikov, C., Stute, M., van Geen, A., 2006. Ensuring safe drinking water in Bangladesh. Science 314, 1687–1688.

Asta, M.P., Kirk Nordstrom, D., Blaine McCleskey, R., 2012. Simultaneous oxidation of arsenic and antimony at low and circumneutral pH, with and without microbial catalysis. Appl. Geochem. 27, 281–291.

Belzile, N., Chen, Y.-W., Wang, Z., 2001. Oxidation of antimony (III) by amorphous iron and manganese oxyhydroxides. Chem. Geol. 174, 379–387.

Buschmann, J., Canonica, S., Sigg, L., 2005. Photoinduced oxidation of antimony (III) in the presence of humic acid. Environ. Sci. Technol. 39, 5335–5341.

Craw, D., Wilson, N., Ashley, P.M., 2004. Geochemical controls on the environmental mobility of Sb and As at mesothermal antimony and gold deposits. Appl. Earth Sci. 113, 3–10.

Daus, B., Wennrich, R., 2014. Investigation on stability and preservation of antimonite in iron rich water samples. Anal. Chim. Acta 847, 44–48.

Fan, J.-X., Wang, Y.-J., Fan, T.-T., Cui, X.-D., Zhou, D.-M., 2014. Photo-induced oxidation of Sb (III) on goethite. Chemosphere 95, 295–300.

Filella, M., Belzile, N., Chen, Y.W., 2002. Antimony in the environment a review focused on natural waters I. Occur. Earth sci. Rev. 57, 125–176.

Filella, M., Belzile, N., Lett, M.-C., 2007. Antimony in the environment: a review focused on natural waters. III. Microbiota relevant interactions. Earth Sci. Rev. 80, 195–217.

Gebel, T., 1997. Arsenic and antimony: comparative approach on mechanistic toxicology. Chem.Biol. Interact. 107, 131–144.

Guo, X., Wu, Z., He, M., Meng, X., Jin, X., Qiu, N., Zhang, J., 2014. Adsorption of antimony onto iron oxyhydroxides: adsorption behavior and surface structure. J. Hazard Mater 276, 339–345.

He, Z., Liu, R., Liu, H., Qu, J., 2015. Adsorption of Sb (III) and Sb (V) on freshly prepared ferric hydroxide (FeOxHy). Environ. Eng. Sci. 32, 95–102.

Hiller, E., Lalinská, B., Chovan, M., Jurkovič, Ľ., Klimko, T., Jankulár, M., Hovorič, R., Šottník, P., Fľaková, R., Ženišová, Z., 2012. Arsenic and antimony contamination of waters, stream sediments and soils in the vicinity of abandoned antimony mines in the Western Carpathians, Slovakia. Appl. Geochem. 27, 598–614.

Leuz, A.-K., Hug, S.J., Wehrli, B., Johnson, C.A., 2006a. Iron-mediated oxidation of antimony (III) by oxygen and hydrogen peroxide compared to arsenic (III) oxidation. Environ. Sci. Technol. 40, 2565–2571.

Leuz, A.-K., Johnson, C.A., 2005. Oxidation of Sb(III) to Sb(V) by O_2 and H_2O_2 in aqueous solutions. Geochim. Cosmochim. Acta 69, 1165–1172.

Leuz, A.-K., Mönch, H., Johnson, C.A., 2006b. Sorption of Sb(III) and Sb(V) to Goethite: influence on Sb(III) oxidation and mobilization. Environ. Sci. Technol. 40, 7277–7282.

McComb, K.A., Craw, D., McQuillan, A.J., 2007. AtrTR-IR spectroscopic study of antimonate adsorption to iron oxide. Langmuir 23, 12125–12130.

Mitsunobu, S., Harada, T., Takahashi, Y., 2006. Comparison of antimony behavior with that of arsenic under various soil redox conditions. Environ. Sci. Technol. 40, 7270–7276.

Oscarson, D.W., Huang, P.M., Defosse, C., Herbillon, A., 1981. Oxidative power of Mn(Iv) and Fe(Iii) oxides with respect to as(Iii) in terrestrial and aquatic environments. Nature 291, 50–51.

Pichler, T., Veizer, J., Hall, G.E., 1999. The chemical composition of shallow-water hydrothermal fluids in tutum Bay, Ambitle Island, Papua New Guinea and their effect on ambient seawater. Mar. Chem. 64, 229–252.

Qi, P., Pichler, T., 2014. Closer look at As(III) and As(V) adsorption onto ferrihydrite under competitive conditions. Langmuir 30, 11110–11116.

Quentel, F., Filella, M., Elleouet, C., Madec, C.-L., 2004. Kinetic studies on Sb (III) oxidation by hydrogen peroxide in aqueous solution. Environ. Sci. Technol. 38, 2843–2848.

Shan, C., Ma, Z., Tong, M., 2014. Efficient removal of trace antimony (III) through adsorption by hematite modified magnetic nanoparticles. J. Hazard Mater 268, 229–236.

Thanabalasingam, P., Pickering, W., 1990. Specific sorption of antimony (III) by the hydrous oxides of Mn, Fe, and Al. Water Air Soil Pollut. 49, 175–185.

Verbinnen, B., Block, C., Lievens, P., Van Brecht, A., Vandecasteele, C., 2013. Simultaneous removal of molybdenum, antimony and selenium oxyanions from wastewater by adsorption on supported magnetite. Waste Biomass Valorization 4, 635–645.

Vink, B., 1996. Stability relations of antimony and arsenic compounds in the light of revised and extended Eh-pH diagrams. Chem. Geol. 130, 21–30.

Vithanage, M., Rajapaksha, A.U., Dou, X., Bolan, N.S., Yang, J.E., Ok, Y.S., 2013. Surface complexation modeling and spectroscopic evidence of antimony adsorption on iron-oxide-rich red earth soils. J. Colloid Interface Sci. 406, 217–224.

Wang, L., Wan, C.-l., Zhang, Y., Lee, D.-J., Liu, X., Chen, X.-f., Tay, J.-H., 2015. Mechanism of enhanced Sb (V) removal from aqueous solution using chemically modified aerobic granules. J. Hazard Mater 284, 43–49.

Wang, X., He, M., Lin, C., Gao, Y., Zheng, L., 2012. Antimony (III) oxidation and antimony (V) adsorption reactions on synthetic manganite. Chem. Erde Geochem. 72, 41–47.

Watkins, R., Weiss, D., Dubbin, W., Peel, K., Coles, B., Arnold, T., 2006. Investigations into the kinetics and thermodynamics of Sb (III) adsorption on goethite (α-FeOOH). J. Colloid Interf. Sci. 303, 639–646.

Wilson, S.C., Lockwood, P.V., Ashley, P.M., Tighe, M., 2010. The chemistry and behaviour of antimony in the soil environment with comparisons to arsenic: a critical review. Environ. Pollut. 158, 1169–1181.

Wu, D., Pichler, T., 2015. Preservation of co-occurring As, Sb and Se species in water samples with EDTA and acidification. Geochem. Explor. Environ. Anal. 15 http://dx.doi.org/10.1144/geochem2015-369.

Xi, J., He, M., Lin, C., 2010. Adsorption of antimony(V) on kaolinite as a function of pH, ionic strength and humic acid. Environ. Earth Sci. 60, 715–722.

Xi, J., He, M., Lin, C., 2011. Adsorption of antimony(III) and antimony(V) on bentonite: kinetics, thermodynamics and anion competition. Microchem J. 97, 85–91.

Xi, J., He, M., Wang, K., Zhang, G., 2013. Adsorption of antimony(III) on goethite in the presence of competitive anions. J. Geochem Explor 132, 201–208.

Xi, J., He, M., Zhang, G., 2014. Antimony adsorption on kaolinite in the presence of competitive anions. Environ. Earth Sci. 71, 2989–2997.

Zhao, X., Dou, X., Mohan, D., Pittman, C.U., Ok, Y.S., Jin, X., 2014. Antimonate and antimonite adsorption by a polyvinyl alcohol-stabilized granular adsorbent containing nanoscale zero-valent iron. Chem. Eng. J. 247, 250–257.

Zhao, Z., Jia, Y., Xu, L., Zhao, S., 2011. Adsorption and heterogeneous oxidation of As(III) on ferrihydrite. Water Res. 45, 6496–6504.